# Mid-Infrared Plasmonic Power Splitters

**Article** *in* IEEE Photonics Technology Letters · November 2016

DOI: 10.1109/LPT.2016.2598272



**2 authors:**

Marina Ayad
The American University in Cairo
**6** PUBLICATIONS **37** CITATIONS
SEE PROFILE

Mohamed A Swillam
The American University in Cairo
**261** PUBLICATIONS **1,569** CITATIONS
SEE PROFILE

# Mid-Infrared Plasmonic Power Splitters

Marina A. Ayad and Mohamed A. Swillam, *Senior Member, IEEE*

***Abstract*— A novel mid-infrared (MIR) plasmonic power splitter is presented. The power splitter is designed initially using an analytic approach. The proposed technique can be extended to 1 × N power splitters. The finite difference time domain technique is utilized to optimize the design. Doped silicon is utilized for the plasmonic effects in the MIR. The proposed power splitter is wideband in the MIR with negligible imbalance. Using the proposed technique, we present 1 × 4, 1 × 8, and 1 × 12 power splitters.**

***Index Terms*— Power splitters, plasmonics, mid-infrared, optical interconnects, photonic modelling.**

## I. Introduction

THE mid-infrared MIR is of great importance in various applications such as optical sensing, thermal signature detection and control and space optical communications [1].

Although the great improvement in enabling the MIR technology by developing efficient sources and detectors yet the rate of the development of the whole infrastructure of optical devices in the MIR is still slow. MIR plasmonics may play an important role in enabling technology in building this infrastructure. The most important motivation for using plasmonics in the visible and near infrared regime is the subwavelength confinement which enabled the development of ultracompact optical interconnects.

However, noble metals behave significantly different in the visible range than its behavior in MIR. The permittivity is negative for wavelengths longer than near ultraviolet. In the visible region, the absolute value of the permittivity is comparable to that of dielectrics. However, in the MIR, the absolute value of Ag permittivity is much larger than that of dielectrics. Consequently, Noble metals act close to perfect conductors in the MIR. At MIR wavelengths, surface plasmon polaritons show high penetration into dielectric and high propagation length. It is advantageous that losses decrease significantly in the MIR. However, this weak confinement hinders the significance of plasmonics.

Transferring the plasmonic applications directly to the MIR is not straightforward since the metals used respond discordantly in these different frequency ranges. Therefore, MIR Plasmonics require new geometries and materials to achieve the subwavelength confinement [2]–[5].

Consequently, finding new material in the MIR is of prime importance. Doped semiconductors can be a useful candidate for MIR plasmonics with plasma wavelengths in the region between 3-30 $\mu$m [1]. The plasma frequency can be controlled through the doping level [6]. One of the main advantage of utilizing doped semiconductors as doped Si and GaAs, is their well understood behavior and manipulation. More importantly, using these materials for plasmonics in MIR will open the door for integration with optoelectronic devices. Doped semiconductors have higher mobility that will give less scattering rate than the noble metals in this spectrum range [7].

Doped semiconductors had been utilized for integrated on-chip applications. Among these components, power splitters are generally one of the key components in any optoelectronic device. It elevates the need of several optical sources on the same chip. Power Splitters in the MIR have not been studied widely. Recently, a power splitter design has been implemented using Graphene Nanoribbon Plasmonics [8]. It was found that the conductivity of the graphene varies depending on the chemical potential that can be controlled by an external electric field. Using the X-junction [9] a four port active power splitter was designed by Graphene Plasmonics and the tunability of the transmission output was dependent of the voltage applied.

Plasmonic Power Splitters in the visible and IR range have been tackled in literature [10]–[14]. Recently an ultracompact wideband power splitter has been designed with minimal imbalance [15]. However, this design was done using metals.

In this letter, we propose novel power splitting devices in a different platform and an easier fabrication process using doped silicon in the MIR range. These devices are compatible with the CMOS technology and allow for good integration with optoelectronics and electronic devices on the same chip. The details of the optimal designs using this technology for various splitting ratio are discussed in the following section.

## II. Optimal Designs

In this case the material has to be changed and the geometries will differ significantly. For the MIR power splitter, a highly doped silicon is used. These designs are utilizing to the plasma model with permittivity $\varepsilon_\infty = 11.7$ F/m, collision frequency $\gamma = 9.464 \times 10^9$ rad/s and plasma frequency $\omega_p = 2.4739 \times 10^{15}$ rad/s. This permittivity is based on a doping of $5\text{x}10^{20}$ cm$^{-3}$ as described in [16] and compared with the experimental measurements in [17].

The design approach utilized in this Power splitter is based on a two stage optimization process. First, using the impedance model to reach an initial design. Second, the Finite Difference Time Domain technique [18] is then utilized to reach the optimum design.

In the following example a 2D simulation is exploited. Perfect Matching Layer (PML) is used to terminate the computational domain with 12 cells in each direction. The simulation time is 10000 time steps with a time step of 0.00283039 f Sec. The mesh size is 3 nm for both the x and y directions. The spatial excitation is done using a modal source which injects the guided mode into the input port.

Manuscript received March 5, 2016; revised July 22, 2016; accepted July 29, 2016. Date of publication August 4, 2016; date of current version October 11, 2016. *(Corresponding author: Mohamed A. Swillam.)*

The authors are with The American University in Cairo, Cairo 11511, Egypt (e-mail: m_ayad@aucegypt.edu; m.swillam@aucegypt.edu).

Color versions of one or more of the figures in this letter are available online at http://ieeexplore.ieee.org.

Digital Object Identifier 10.1109/LPT.2016.2598272

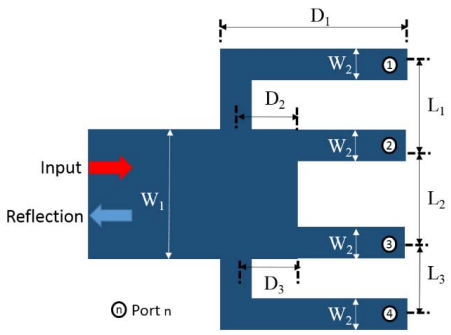


Fig. 1. Optimum 1×4 Power Splitter Schematic with uppermost arm labeled as Port 1.

### A. 1 × 4 Power Splitter

To design a $1 \times 4$ power splitter, this will require five ports where one port is the input port and the rest four ports are the output ports. The design should be done in order not to have any reflection from the input port. In this design the transmission from each output port is equal so the expected transmission from each port is 25 %. Using the impedance model the input port's impedance is the summation of the widths of the output ports $Z_1 = Z_2+Z_3+Z_4+Z_5$ where all the output ports have the same impedance $Z_2 = Z_3 = Z_4 = Z_5$, consequently, all the output ports have the same widths. Using the FDTD commercial tool [16] the optimization problem is solved to get the optimum design with minimal imbalance. The design parameter vector is $p = [W_1\ W_2\ L_1\ L_2\ L_3\ D_1\ D_2\ D_3]$.

The input arm's width $W_1$ is 0.8 $\mu$m, therefore the four output arm's widths are 0.2 $\mu$m. The monitors are put on the edge with $D_1 = 0.95$ $\mu$m. $D_2$ and $D_3$ are the distances from the midpoint of the arms to the edge of the input arm as shown in Figure 1. These parameters have a strong effect on the results since they are the first two arms facing the source. If they are put too close from the source most of the power will be given to them as it will take a longer path to reach the rest of the ports. Another cause of their importance is resultant from the bend in the light paths of Port 1 and Port 2. The light path in these two ports are longer therefore the losses may increase. Therefore a good compromise has to be done in positioning Port 1 and Port 4 to reach minimal losses. The FDTD software is used to solve the optimization problem. LB and UB are the vectors that contain the lower and upper bounds of all the design parameters. This problem is solved with LB set as 0.1$\mu$m and UB set as 0.95 $\mu$m and it was found that $D_2 = D_3 = 0.24$ $\mu$m. Also the FDTD is used to determine $L_1$, $L_2$ and $L_3$. Since symmetry was found to be optimal therefore $L_1$ is equal to $L_3$. Due to symmetry the transmissions from ports 1 and 4 are equal to the transmissions from ports 2 and 3. Using this idea $L_1 = L_3 = 0.425$ $\mu$m and $L_2 = 0.6$ $\mu$m. The transmission results are as expected around 25 % as an average value with a maximum reflection of <0.025%. The impedance model in this design is achievable in the range of wavelengths from 5 $\mu$m till 10 $\mu$m. As shown in Figure 2 the imbalance reached in this model is approximately 1% and the reflection at the input port is negligible in comparison with the results. The field intensity at wavelength $\lambda = 5$ $\mu$m is shown in Fig. 3 where equal division of the intensity between the four output ports is shown. The footprint of the device

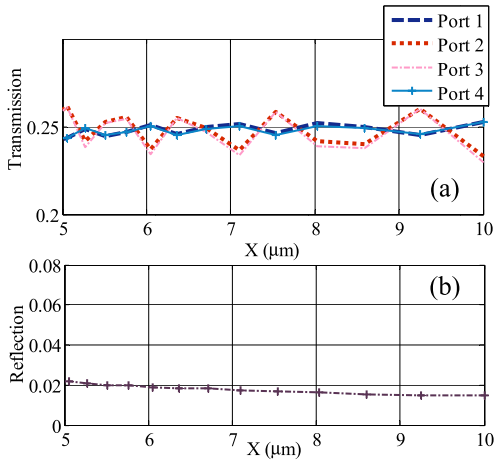


Fig. 2. (a) Transmission of 1×4 Power Splitter. (b) Reflection.

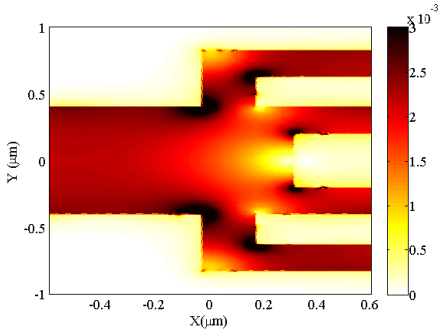


Fig. 3. Field Intensity at $\lambda = 5$ $\mu$m.

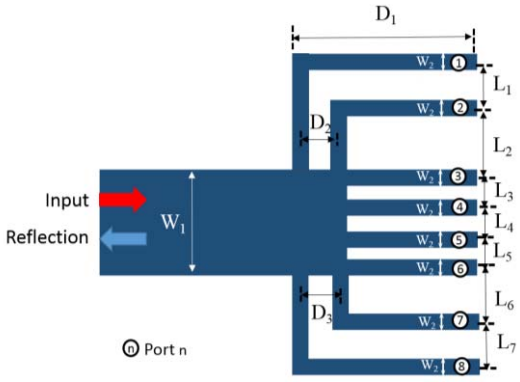


Fig. 4. Optimum $1 \times 8$ Power Splitter Schematic with uppermost arm labeled as Port 1.

is 1.2 $\mu$m × 1 $\mu$m and the results hold for a wideband of wavelengths.

### B. 1 × 8 Power Splitter

Again using the impedance model the power splitter design is extended to a 1×8 Power Splitter. However, the optimization problem here is with higher difficulty. The expected output power transmission is 12.5 %. The input port's width $W_1$ is 0.8 $\mu$m and by dividing this width by 8, each output port's width $W_2$ is 0.1 $\mu$m. The vector of design parameters is $p = [W_1\ W_2\ D_1\ D_2\ D_3\ L_1\ L_2\ L_3\ L_4\ L_5\ L_6\ L_7]$. The schematic of the design is shown in Figure 4. The design contains of four arm distributed up and down from the input port. The symmetric approach is similarly used in this design imposing $D_2 = D_3$, $L_1 = L_7$, $L_2 = L_6$ and $L_3 = L_5$.

TABLE I
1 × 8 PARAMETER VALUES

| Parameter | Value (μm) |
|---|---|
| $W_1$ | 0.8 |
| $W_2$ | 0.1 |
| $D_1$ | 0.42 |
| $D_2$,$D_3$ | 0.13 |
| $L_1$,$L_7$ | 0.2 |
| $L_2$,$L_6$ | 0.21 |
| $L_3$,$L_5$ | 0.25 |
| $L_4$ | 0.2 |

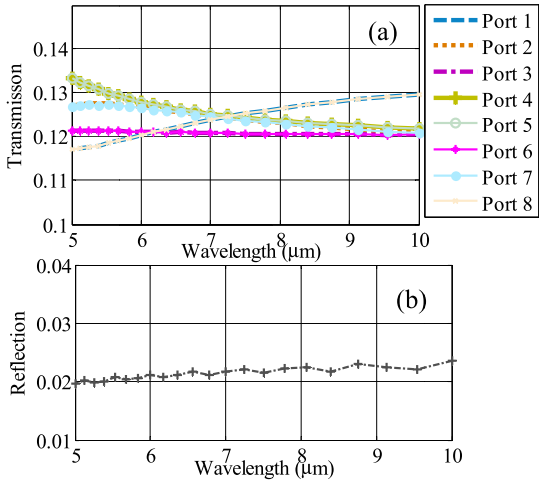


Fig. 5. (a) Transmission of 1 × 8 Power Splitter. (b) Reflection.

This symmetry will cause equivalent transmission outputs from Ports 1 and 8, Ports 2 and 7, Ports 3 and 6, Ports 4 and 5.

The first step in the design was accomplished using the impedance model where the widths of the input and output ports were determined. The next step is using the FDTD to solve the optimization problem and reach the minimum possible imbalance. The optimization problem was solved with LB of 0.1 $\mu$m and an UB of 0.8 $\mu$m. The optimum values for the design parameters are shown in Table I.

As shown in Figure 5 the transmission is about 12.5% as expected for a range of wavelengths from 5 $\mu$m till 10 $\mu$m. The imbalance is about 1%. Similarly $D_2$ and $D_3$ have a high impact on the output transmission. A sweep was done on the values of $D_2$ and $D_3$ from 0.28 $\mu$m till 0.12 $\mu$ m and it was found that the imbalance in this case varies from approximately 2.5% till 1%. So it is shown that the closer the ports are from each other the less the imbalance will be. Another sweep was done on the values on the values of $L_3$and$L_5$, eventually varying the value of $L_4$, from 0.15 till 0.25 the imbalance reaches 2.5 % and decreases with the increase of the values of $L_3$ and $L_5$ till it reaches 1 %.

The field intensity is shown in Figure 6 where equal intensity is shown. The footprint of the device is 1.2 $\mu$ m×1 $\mu$m and the results hold for a wideband of wavelengths.

### C. 1×12 Power Splitter:

The 1×12 Splitter is done similarly. However, this design is much more challenging in implementation. The first trial is done similar to the 1×8 design by putting 4 output ports on the upper and lower side of the input port and the rest of the 8 arms were put on the rear end of the input port. The input port has width 1.2 $\mu$m therefore, using the impedance model for equal division between the 12 output ports, the output ports' width is 0.1 $\mu$m. The optimization problem is solved using the FDTD software to find optimum values for the vector of design parameters, p = [$W_1$ $W_2$ $D_1$ $D_2$ $D_3$ $L_1$ $L_2$ $L_3$ $L_4$ $L_5$ $L_6$ $L_7$ $L_8$ $L_9$ $L_{10}$ $L_{11}$]. The LB for the optimization problem is 0.1 $\mu$m and the UB is 1.2 $\mu$m. The schematic for the first approach design is shown in Figure 7. Similar as the previous examples symmetry is used in the design. The symmetry is achieved using $L_1 = L_{11}$, $L_2 = L_{10}$, $L_3 = L_9$, $L_4 = L_8$, $L_5 = L_7$ and $D_2 = D_3$. This symmetry will cause equivalent transmission outputs from Ports 1 and 12, Ports 2 and 11, Ports 3 and 10, Ports 4 and 9, Ports 5 and 8, Ports 6 and 7. The parameters calculated by the FDTD are shown in Table II. The simulation requires 11 minutes on a quad core processor.

A sweep was done on the values of the parameters. However, some parameters have a higher effect on the performance than others. For example, varying $L_6$ from 0.2 $\mu$m to 0.14 $\mu$m didn't do any noticeable change in the transmission values. However, varying $D_2$ and $D_3$ from 0.33 $\mu$m to 0.16 $\mu$m the imbalance reaches to 2.6 % at 0.33 $\mu$m. The maximum imbalance reached in case of optimum values is 1.3 % and the error decreases to less than 1 % at higher wavelengths as

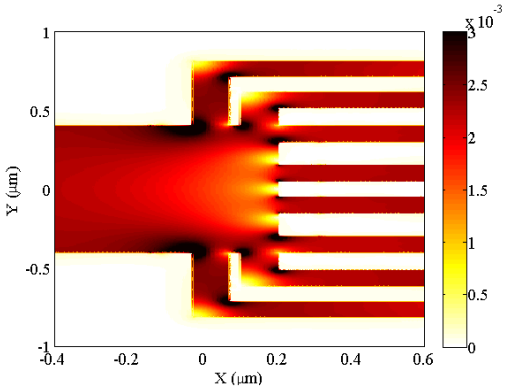


Fig. 6. Field Intensity of 1 × 8 at $\lambda = 5$ $\mu$m.

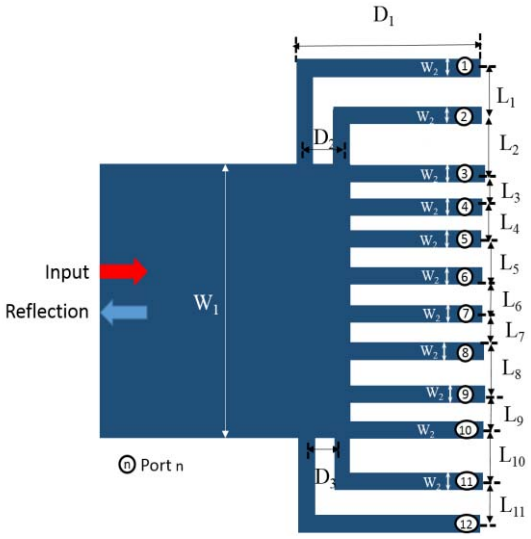


Fig. 7. 1 × 12 First Approach Power Splitter Schematic with uppermost arm labeled as Port 1.

TABLE II
FIRST APPROACH 1 × 12 POWER SPLITTER OPTIMUM PARAMETERS

| Parameter | Value (μm) |
|---|---|
| $W_1$ | 1.2 |
| $W_2$ | 0.1 |
| $D_1$ | 0.35 |
| $D_2$,$D_3$ | 0.18 |
| $L_1$,$L_{11}$ | 0.15 |
| $L_2$,$L_{10}$ | 0.15 |
| $L_3$,$L_9$ | 0.15 |
| $L_4$,$L_8$ | 0.15 |
| $L_5$,$L_7$ | 0.18 |
| $L_6$ | 0.14 |

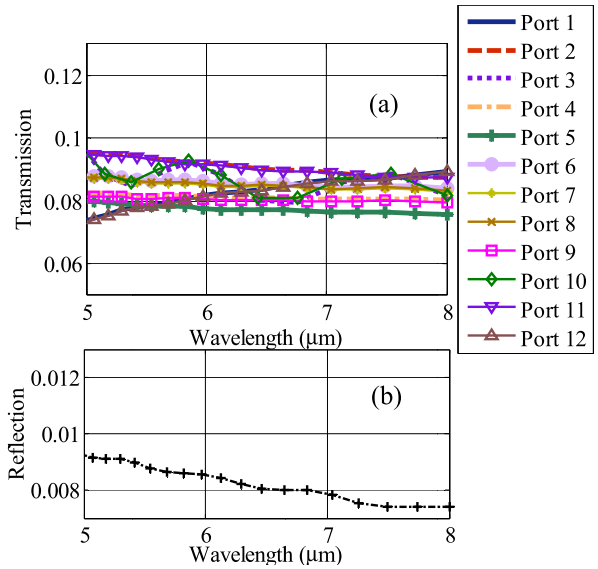


Fig. 8. (a) Transmission of 1 × 12 First Approach Power Splitter. (b) Reflection.

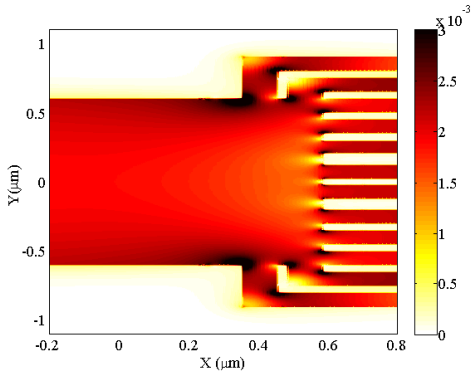


Fig. 9. Field Intensity of 1 × 12 first Approach Power Splitter.

shown in Figure 8. The field intensity is shown in Figure 9 where equal intensity is shown.

The output arms can be further separated using sharp "L" bends to avoid any coupling between the output ports. This sharp bends will allow for achieving large separation over small distances, compared with the conventional "S" bend utilized in conventional photonics.

## III. CONCLUSION

A MIR plasmonic power splitter is proposed using doped silicon. For the first time an analytic approach was utilized to obtain the initial design of a 1×N MIR plasmonic power splitter. The optimization was developed using FDTD approach. The methodology is demonstrated through proposing optimal design of 1 × 4, 1 × 8 and 1 × 12 power splitter.

## REFERENCES

[1] S. Law, V. Podolskiy, and D. Wasserman, "Towards nano-scale photonics with micro-scale photons: The opportunities and challenges of mid-infrared plasmonics," *Nanophotonics*, vol. 2, no. 2, pp. 103–130, 2013. [Online]. Available: http://www.degruyter.com/view/j/nanoph.2013.2.issue-2/nanoph-2012-0027/nanoph-2012-0027.xml, doi: 10.1515/nanoph-2012-0027.

[2] K. S. Novoselov *et al.*, "Electric field effect in atomically thin carbon films," *Science*, vol. 306, no. 5696, pp. 666–669, 2004. [Online]. Available: http://www.jstor.org/stable/3839379

[3] K. S. Novoselov *et al.*, "Two-dimensional atomic crystals," *Proc. Nat. Acad. Sci. USA*, vol. 102, no. 30, pp. 10451–10453, 2005. [Online]. Available: http://www.jstor.org/stable/3376103

[4] F. H. L. Koppens, D. E. Chang, and F. J. G. de Abajo, "Graphene plasmonics: A platform for strong light–matter interactions," *Nano Lett.*, vol. 11, no. 8, pp. 3370–3377, 2011. [Online]. Available: http://dx.doi.org/10.1021/nl201771h, doi: 10.1021/nl201771h.

[5] A. N. Grigorenko, M. Polini, and K. S. Novoselov, "Graphene plasmonics," *Nature Photon.*, vol. 6, no. 11, pp. 749–758, 2012. [Online]. Available: http://search.ebscohost.com/login.aspx?direct=true&db=a9h&AN=83140092&site=ehost-live, doi: 10.1038/nphoton.2012.262.

[6] A. Boltasseva and H. A. Atwater, "Low-loss plasmonic metamaterials," *Mater. Sci.*, vol. 331, no. 6015, pp. 290–291, Jan. 2011, doi: 10.1126/science.1198258.

[7] J. B. Khurgin and A. Boltasseva, "Reflecting upon the losses in plasmonics and metamaterials," *MRS Bull.*, vol. 37, no. 8, pp. 768–779, 2012. [Online]. Available: http://dx.doi.org/10.1557/mrs.2012.173, doi: 10.1557/mrs.2012.173.

[8] K. J. A. Ooi, H. S. Chu, L. K. Ang, and P. Bai, "Mid-infrared active graphene nanoribbon plasmonic waveguide devices," *J. Opt. Soc. Amer. B*, vol. 30, no. 12, pp. 3111–3116, 2013. [Online]. Available: http://josab.osa.org/abstract.cfm?URI=josab-30-12-3111, doi: 10.1364/JOSAB.30.003111.

[9] E. Feigenbaum and M. Orenstein, "Perfect 4-way splitting in nano plasmonic X-junctions," *Opt. Exp.*, vol. 15, no. 26, pp. 17948–17953, 2007. [Online]. Available: http://www.opticsexpress.org/abstract.cfm?URI=oe-15-26-17948, doi: 10.1364/OE.15.017948.

[10] G. Veronis and S. Fan, "Bends and splitters in metal-dielectric-metal subwavelength plasmonic waveguides," *Appl. Phys. Lett.*, vol. 87, no. 13, p. 131102, 2005. [Online]. Available: http://dx.doi.org/10.1063/1.2056594

[11] J. Wang *et al.*, "Sub-$\mu$m$^2$ power splitters by using silicon hybrid plasmonic waveguides," *Opt. Exp.*, vol. 19, no. 2, pp. 838–847, 2011, doi: 10.1364/OE.19.000838.

[12] M. A. Swillam, M. H. Bakr, and X. Li, "Efficient 3D sensitivity analysis of surface plasmon waveguide structures," *Opt. Exp.*, vol. 16, no. 21, pp. 16371–16381, 2008, doi: 172420.[pii].

[13] N. Nozhat and N. Granpayeh, "Ultra-compact metal-insulator-metal plasmonic power splitter at 1550 nm wavelength," presented at the Photon. Global Conf. (PGC), Dec. 2010, pp. 1–4, doi: 10.1109/PGC.2010.5706081.

[14] P. Dastmalchi, N. Granpayeh, and M. R. Disfani, "Three-dimensional gap plasmon power splitters suitable for photonic integrated circuits," *Opt. Quantum Electron.*, vol. 42, no. 4, pp. 231–239, Mar. 2010. [Online]. Available: http://dx.doi.org/10.1007/s11082-011-9448-9, doi: 10.1007/s11082-011-9448-9.

[15] M. A. Ayad, S. S. A. Obayya, and M. A. Swillam, "Submicron 1xN ultra wideband MIM plasmonic power splitters," *J. Lightw. Technol.*, vol. 32, no. 9, pp. 1814–1820, May 1, 2014, doi: 10.1109/JLT.2014.2312673.

[16] R. Gamal, Y. Ismail, and M. A. Swillam, "Silicon waveguides at the mid-infrared," *J. Lightw. Technol.*, vol. 33, no. 15, pp. 3207–3214, Aug. 1, 2015, doi: 10.1109/JLT.2015.2410493.

[17] E. D. Palik, Ed., *Handbook of Optical Constants of Solids*, vol. 3. New York, NY, USA: Academic, 1998, ch. 6.

[18] *Lumerical*, acessed on 2015. [Online]. Available: http://www.lumerical.com/solutions/whitepapers/fdtd_multicoefficient_material_modeling.html